



## Determination of angle of impact and directionality of drip stains on various fabrics

Dylan J. Drazdik<sup>a</sup>, David M. Hammond<sup>b</sup>, Travis J. Worst<sup>a</sup>, Crystal M. Oechsle<sup>a,\*</sup>

<sup>a</sup> Ohio Attorney General's Center for The Future of Forensic Science, Bowling Green State University, Bowling Green, OH 43403, USA

<sup>b</sup> Ohio Bureau of Criminal Investigation, Crime Scene Unit, 750 N. College Drive, Bowling Green, OH 43402, USA

### ARTICLE INFO

#### Keywords:

Bloodstain pattern analysis  
Fabric  
Bloodstain morphology  
Angle of impact  
Directionality  
Wicking

### ABSTRACT

Bloodstain pattern analysis (BPA) on absorbent surfaces, such as fabrics, is far more complex compared to its application on smooth, hard, non-porous surfaces. Angle of impact and directionality are commonly interpreted from bloodstains but may be adversely affected by porous surfaces. In fact, there is a lack of evidence that traditional approaches to BPA are even applicable when blood impacts absorbent materials such as clothing and other fabrics. Hence, there is a critical need for research focusing on the validity and reliability of methods for bloodstain pattern analysis on textiles. Here, human blood drops were deposited on six different fabric types (cotton, satin polyester, rayon, blended polyester/spandex, blended nylon/spandex, and blended modal/polyester/spandex) at two known impact angles: 30° and 10°. Bloodstain morphology was found to be unique for each fabric. Calculated angles of impact for cotton and satin polyester were not statistically different from the known angle of impact while blended polyester/spandex, blended nylon/spandex, and blended modal/polyester/spandex significantly underestimated the known angle of impact. Even when stain morphology on fabric resembled those on a glass control, the angle of impact significantly underestimated the known. The ability to assign directionality based upon bloodstain morphology was dependent on the fabric type. These findings support the need for further research and the development of guidelines for bloodstain pattern interpretation on fabric materials.

### 1. Introduction

Bloodstain pattern analysis (BPA) is based on observations of the physical characteristics that bloodstains exhibit and is, therefore, one of the more subjective disciplines within the field of forensic science. Difficulties arise when interpreting bloodstains on porous materials because the stages of impact differ when a blood droplet impacts a porous, absorbent surface, primarily due to contours of the surface and wicking. Wicking is the movement of a liquid within a porous material driven by capillary forces. Wang et al. [1] examined the process of droplet formation and wicking on fabrics, classifying four different stages: inertial impact, absorption, first wicking, and second wicking. During the inertial impact stage, the blood droplet shape is disbanded, and blood radiates outward. Blood is absorbed vertically during the absorption phase, then, in the wicking stages, blood spreads radially and increases the diameter of the stain. Wicking in the first stage happens uniformly but is more irregular in the second wicking stage. These

complex interactions lead to interpretation difficulties when bloodstains are deposited on fabrics.

Elliptical stains, typically seen if blood impacts a surface at an angle, are caused by the blood droplets skidding across the substrate before immobilizing. As blood first contacts a surface, a smooth leading edge is formed, whereas spines, tapering, and tails are produced by inertial forces at the terminal edge of a bloodstain (Fig. 1). The direction the blood was traveling at the time of impact can be determined from the direction the terminal edge is pointing [2]. The final shape of elliptical stains is related to the degree of the angle at which blood impacted the surface. The ratio between the outward motion of a bloodstain, or width (W) at the widest point, and the forward motion, or length (L) at the longest point excluding the tail, of a stain is described by a trigonometric relationship with the angle of impact. With these two parameters, width and length, the angle of impact can be estimated using the equation,  $\sin\theta = \frac{W}{L}$ . White [3] presented evidence to suggest that the trigonometric equation for calculating an angle of impact on fabric was not

\* Correspondence to: Ohio Attorney General's Center for The Future of Forensic Science, Bowling Green State University, 116 Life Science Building, Bowling Green, OH 43403, USA.

E-mail address: [coechsl@bgsu.edu](mailto:coechsl@bgsu.edu) (C.M. Oechsle).

<https://doi.org/10.1016/j.forensiint.2024.112096>

Received 11 March 2024; Received in revised form 23 May 2024; Accepted 5 June 2024

Available online 6 June 2024

0379-0738/© 2024 The Author(s). Published by Elsevier B.V. This is an open access article under the CC BY-NC-ND license (<http://creativecommons.org/licenses/by-nc-nd/4.0/>).

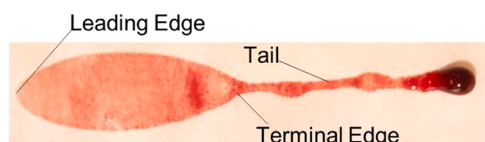


Fig. 1. Quintessential blood impact stain morphology. Bloodstain formed from human blood impacting butcher paper at a known 30° angle.

reliable. However, if second stage wicking irregularities –

such as spines, edge distortion, and obvious wicking (blood following along a yarn outside the bulk of the bloodstain) – are excluded, perhaps a trigonometric equation may be applicable. Estimating an angle of impact and interpreting a directionality is important to BPA because they are necessary for determining an area of origin, which may provide valuable information on where the bleeder was located and how they were oriented in relation to the scene and/or objects when the bloodstain deposition occurred [2].

Research on the interaction between blood and textiles is still in its infancy. The effects of fabric composition on bloodstain formation and morphology have generally been limited to cotton [1,4–6], polyester [7], and denim [8]. While studies have been conducted and guidelines implemented for interpretations on cotton, polyester, and denim [9], a comparison of bloodstain morphology across a larger number of fabric substrates has not yet been performed, which leaves a gap of knowledge because of the wide array of common textiles, like spandex, that have not yet been evaluated. A critical need for research into the interaction between blood and textiles which could aid in the development BPA standards has been formally recognized [10]. Understanding how blood interacts with various fabric types will help examiners determine when reliable information can, and cannot, be derived from bloodstains on a particular textile. Although it should be noted that a textile or garment may have folds, intentional or otherwise, and twists, which also complicate the classification of patterns and the analysis that can be made of them, understanding of how blood interacts with these porous and absorbent materials will improve the accuracy and reliability of how bloodstain patterns on textiles will be interpreted [11]. In this study, the effect of fabric substrate on bloodstain morphology, elliptical area, angle of impact, and directionality was compared between and extended to additional fabric types, including cotton, satin polyester, rayon, blended polyester/spandex, blended nylon/spandex, and blended modal/polyester/spandex.

## 2. Materials & methods

### 2.1. Blood source and fabrics

One pint of single donor, human, whole blood with added lithium heparin anticoagulant was purchased from Innovative Research (Novi, MI). Pursuant to FDA regulations, the human whole blood was held for viral testing by Innovative Research before being shipped (chilled, on gel packs), and the blood was received two days after being drawn. Blood was refrigerated at 7 °C, per product instructions, until use. A variety of white fabrics were obtained. Single knit polyester/spandex blend (95 % polyester, 5 % spandex) – henceforth referred to as “poly/span”, satin polyester (100 % polyester) – henceforth referred to as “polyester”, and plain-woven cotton (100 % cotton) – henceforth referred to as “cotton” – fabrics were purchased from Hobby Lobby (Perrysburg, OH). Single knit nylon/spandex blend (75 % nylon, 25 % spandex) – henceforth referred to as “nylon”, single knit modal blend (67 % modal, 28 % polyester, 5 % spandex) – henceforth referred to as “modal”, and plain-woven rayon (100 % rayon) – henceforth referred to as “rayon” – fabrics were purchased from Joann Fabrics (Toledo, OH). The structure of each fabric was verified using a Lieca EZ4 stereomicroscope (Serial #6063006) under 35x magnification and reflected light. All fabrics were laundered once prior to use according to the

manufacturer recommendations (Table 1) and using Tide Original detergent (Procter & Gamble, USA). Machine laundering occurred using a SpeedQueen Commercial Washer (Model #SWNNC2SP115TW01) while machine drying occurred using a SpeedQueen Commercial Dryer (Model #SDGNCRGS113TW01).

### 2.2. Drip stain apparatus

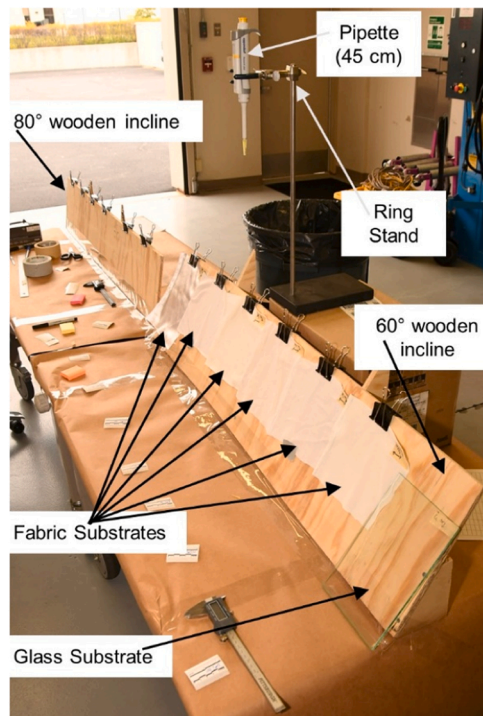
A wooden apparatus (Fig. 2) was constructed with two wooden planks mounted on wooden ramps to produce either 30° or 10° impact angles when the blood droplets hit the substrate from the vertical direction. Each of the six fabrics were cut into five replicate 18 cm×18 cm squares and labeled with the fabric type, the weft (crosswise running yarns in woven fabric) or course (crosswise running yarns in knit fabric) direction, the known impact angle, and the direction of blood travel. Fabric squares were secured onto the wooden plank with the weft or course yarns running horizontally in the same direction. Because glass is a smooth, hard, and non-porous surface capable of producing quintessential drip stains, a square of glass was used as a substrate control and was leaned against the wooden apparatus such that the glass was in close contact with the wood (Fig. 2). A 200 µL Research Plus micropipette (Eppendorf) was mounted to a ring stand ~ 45 cm above the center of the wooden plank. Following the procedure described by Chang and Michielsen [12] to consistently release a volume of blood as a spherical droplet, 200 µL Fisherbrand micropipette tips (Thermo Fisher Scientific) were modified by removing 2 cm from the pipette tip with a scalpel. On the day of use, the blood was allowed to equilibrate to ambient temperature (~70 °F; ~21°C) and mixed by inversion periodically prior to use. To produce each replicate drop, 50 µL of blood was measured by pipette and dispensed using a modified tip, creating a bloodstain on the target substrate. After impact, the bloodstain was immediately photographed (T = 0) with a Nikon D500 camera. Then, an adhesive scale was placed next to the bloodstain, which was then photographed a second time (T = 0 + Scale). Each of the substrates were removed from the apparatus and left to dry flat on clean butcher paper for thirty minutes after which, all bloodstains were photographed a third time (T = +30 Min). Thirty minutes was chosen to allow for wicking and absorption that would better mimic the inevitable time delay between a deposition event and observation that is extremely variable but inherent in crime scene investigation.

### 2.3. Angle of impact and area

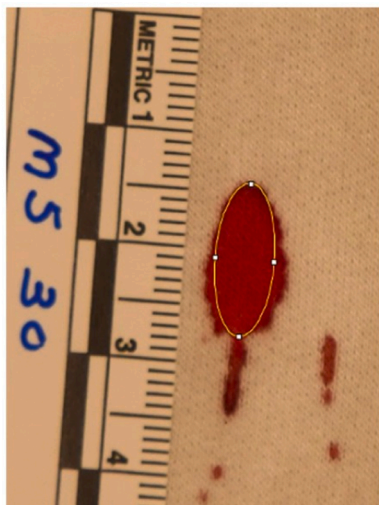
All photographs of bloodstains taken after 30 minutes of drying were analyzed using the ImageJ software (imagej.net/ij/, version 1.53 t), which is a freeware available from the National Institute of Health (NIH). In ImageJ, an ellipse was added to the photograph to best encompass the bloodstain while excluding obvious wicking, edge distortion, spines, and tails from the area of the ellipse (Fig. 3). Measurements of the major axis and minor axis for each ellipse were recorded. Using the major axis as the length (L) and the minor axis as the width (W), an angle of impact was calculated for each bloodstain. As an indication of accuracy, percent error for each angle of impact was derived in reference to the known impact angle. As an indication of precision, relative standard deviation (RSD) was derived from the mean

Table 1  
Laundering and drying conditions for the six tested fabric substrates.

Fabrics	Laundering Conditions	Drying Conditions
Cotton & Modal	30-minute run cycle, cold water temperature setting with agitation	45-minute run cycle, low temperature setting
Polyester & Poly/Span	30-minute run cycle, warm water temperature setting with agitation	45-minute run cycle, low temperature setting
Rayon & Nylon	Hand-washed and soaked in cold water for 30 minutes	Air-dried for 24 hours



**Fig. 2.** Drip stain apparatus. Fabric swatches were mounted to, and the glass pane rested up against, the 60° wooden incline in the foreground to create the known 30° impact angle stains. A 50  $\mu$ L droplet of human blood was dispensed from the pipette 45 cm above the substrates. The same experimental procedure was then repeated for the 80° wooden incline (seen in the background) to create the known 10° impact angle stains.



**Fig. 3.** Elliptical selection of a bloodstain in ImageJ. Representative screenshot from ImageJ software depicting elliptical selection (yellow outline) of a bloodstain deposited on modal fabric. Length of the ellipse (major axis) ends before the tail of the bloodstain begins. Width of the ellipse (minor axis) encompasses as much of the bloodstain as possible without the ellipse passing outside the bounds of the bloodstain, negating uneven edge distortion.

angle of impact and the standard deviation for each substrate at a specific impact angle. To compare how stain size may differ between fabric and glass substrates, the area of each ellipse was calculated by the equation,  $A = \pi(0.5(\text{major axis}))(0.5(\text{minor axis}))$ .

## 2.4. Directionality

All photographs analyzed for angle of impact were cropped to remove the scale, edge of fabric, or any other identifying information so that only the bloodstain in question and any satellite stains were visible. Each cropped photograph was uploaded to a document and randomly oriented. Directionality was determined by a certified bloodstain pattern analyst who had 200 hours of training related to bloodstain pattern analysis and 22 years of crime scene investigation experience. The analyst provided an opinion for all photographs as to the direction the blood was traveling before impact with regard to the orientation in the photograph (up, down, left, right, or unable to determine). Bloodstains that were assigned a directionality by the examiner were used to determine accuracy by comparing to the original photograph and the ground-truth of the direction the blood was traveling prior to impact.

## 2.5. Data analysis

Additional analysis of data was performed in Microsoft Excel (version 2308), as needed. Statistical analysis of data was performed using the R software package (r-project.org, version 4.3.1). For each fabric type, the mean angle of impact was compared to the known angle of impact, either 10° or 30°, in a single sample t-test. The Shapiro-Wilk Test for Normality was conducted to determine the distribution of the angle of impact and elliptical area data, and each dataset demonstrated skewed distributions. As datasets were non-parametric, the Kruskal-Wallis rank sum test was used to compare mean angles of impact and elliptical areas among the different substrate types at each of the two known angles of impact (10° and 30°). Significant differences, if any, were then confirmed using Dunn Test for multiple comparisons. To determine if a dependent relationship existed between the substrate type and the ability to derive a directionality from a bloodstain, a chi-squared test of independence was needed to analyze the nominal data (i.e., could directionality be accurately determined? ‘yes’ or ‘no’); a Fisher’s exact test was substituted for a chi-squared test of independence due to unbalanced and small sample sizes in this study. The number of stains assigned a directionality classification (observed) were organized into a table. Columns were divided by substrate type and rows were divided by directionality classification (either classified or not classified). Using the data from this table, the expected number of stains were calculated by the following equation,  $Expected\ value = \frac{(\text{row total} \times \text{column total})}{\text{total observations}}$ . The Fisher’s exact test compared the observed number of directionality classifications to the derived expected number of classifications for the 30° impact angle and the 10° impact angle.

## 3. Results

### 3.1. Bloodstain appearance

Bloodstains on polyester, poly/span, cotton, modal, rayon, and nylon fabrics were visually distinct from one another. Fig. 4 shows different bloodstain morphology across various fabrics under the same, 30° known, impact conditions. Bloodstains on the polyester fabric (Fig. 4A) resulted in a red band of blood surrounded by a faint, more elliptical area of blood caused by wicking (Fig. 5). Bloodstains on the poly/span fabric also had an area of a faint red color with specks of a deeper red color within the elliptical shape. However, on poly/span fabric, blood tended not to be absorbed but form small, spherical drops that could roll across the substrate with gravity (Fig. 4B). In contrast, cotton fabric (Fig. 4C) seemed to demonstrate a higher degree of absorptivity and wicking (Fig. 6), creating bloodstains with unsymmetric shapes and irregular edge distortion. Polyester (Fig. 5) and cotton (Fig. 6) fabrics demonstrated a greater wicking ability over time compared to the other fabric substrates, as demonstrated by the shape observed in the first photograph (immediately after impact) compared to the shape observed

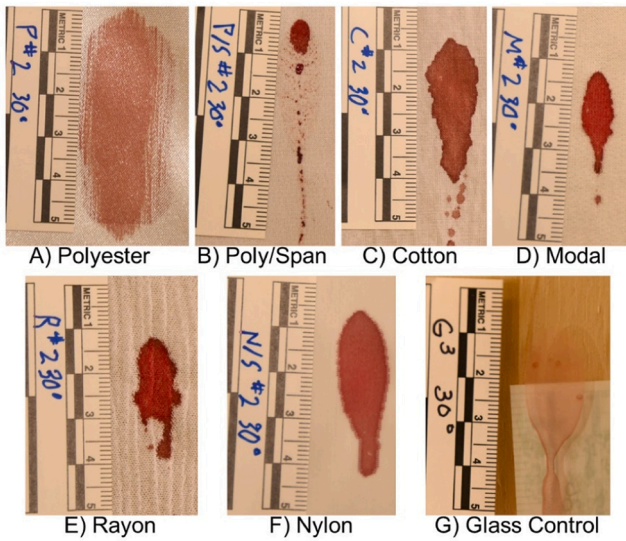


**Fig. 4.** Representative bloodstain morphologies for known 30° impact stains across fabric types. Images were captured after 30 minutes of drying. A) Polyester (top left); B) Polyester/spandex blend or ‘poly/span’ (top middle-left); C) Cotton (top middle-right); D) Modal (top right); E) Rayon (bottom left); F) Nylon (bottom middle); and G) Glass Control (bottom right).

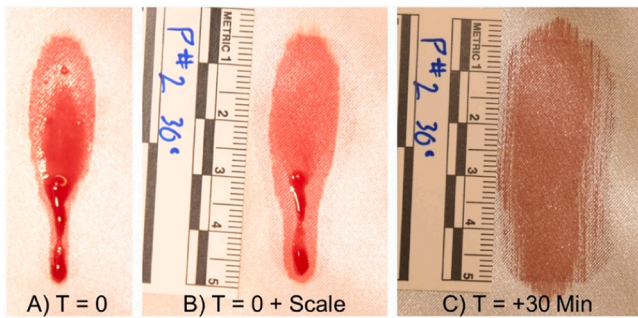


**Fig. 5.** Representative blood drip stain morphologies on polyester fabric over time for known 30° impact. Photographs taken A) immediately after impact (T = 0), B) after an adhesive scale was placed (T = 0 + Scale), and C) 30 minutes after impact (T = +30 Min).

in the last photograph (30 minutes of drying) of each stain. Both the modal (Fig. 4D) and rayon (Fig. 4E) fabrics created smaller bloodstains compared to the other substrates. The nylon fabric (Fig. 4F) had bloodstains that most resembled the bloodstains on glass (Fig. 4G), demonstrating the expected morphology seen in Fig. 1. However, the edges of the bloodstains on nylon fabric (Fig. 4F) often showed obvious wicking in the course direction of the fabric.

Bloodstains impacting at a known 10° angle (Fig. 7) were comparatively more elongated than those impacting at 30° angles (Fig. 4), as expected, but stains at a known 10° angle also demonstrated different morphologies across various fabric types. At this more acute angle, the polyester fabric (Fig. 7A) demonstrated a more elliptical appearance and had a distinctive tail in most instances; a faint area of blood could still be seen surrounding the prominent portion of the bloodstain. The poly/span fabric (Fig. 7B) formed faint stains with smaller, undisturbed blood droplets resting on the top of the fabric surface. Often, these droplets would roll down the fabric, creating a bloodstain trail. Cotton (Fig. 7C) created bloodstains of varying, irregular shapes. The modal fabric (Fig. 7D) created stains with jagged and sharp edges. The rayon fabric (Fig. 7E) created bloodstains with edge distortion and asymmetric tails. Again, the nylon fabric (Fig. 7F) had bloodstains that most resembled the bloodstains on glass (Fig. 7G); however, obvious wicking could be

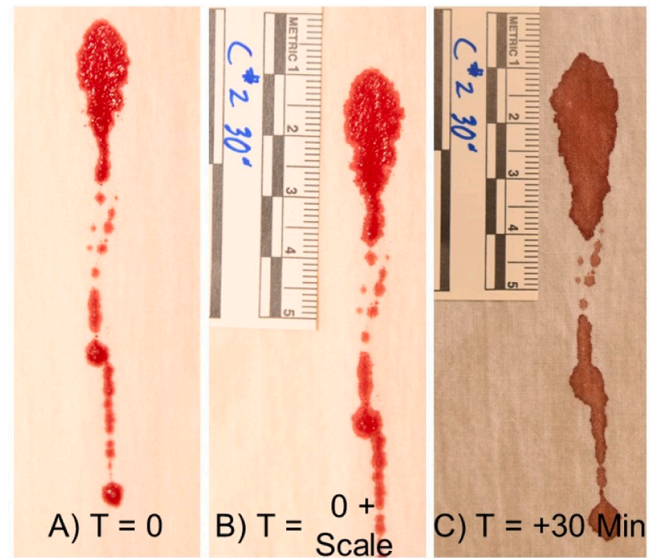


**Fig. 6.** Representative blood drip stain morphologies on cotton fabric over time for known 30° impact. Photographs taken A) immediately after impact (T = 0), B) after an adhesive scale was placed (T = 0 + Scale), and C) 30 minutes after impact (T = +30 Min).

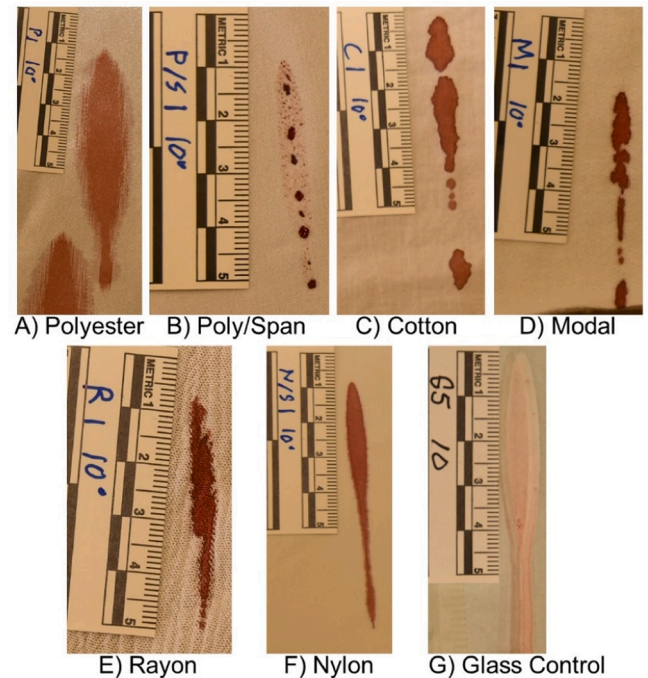


**Fig. 7.** Representative bloodstain morphologies for known 10° impact stains across fabric types. Images were captured after 30 minutes of drying. A) Polyester (top left); B) Polyester/spandex blend or ‘poly/span’ (top middle-left); C) Cotton (top middle-right); D) Modal (top right); E) Rayon (bottom left); F) Nylon (bottom middle); and G) Glass Control (bottom right).

seen as ‘fuzzy’ edges around the bloodstain, mostly in the course direction of the knit fabric. Like the 30° impacts, the polyester and cotton fabrics demonstrated a greater ability of blood wicking over time from impact to thirty minutes after (data not shown).

### 3.2. Elliptical area

The mean bloodstain size based on the area of the ellipse (Fig. 3)

ranged from 60.1 mm<sup>2</sup> to 454.3 mm<sup>2</sup> across the various fabric substrates, with modal fabric yielding the smallest stains and polyester fabric yielding the largest stains (Table 2). Except for polyester, the fabrics stains had mean elliptical areas less than the mean elliptical area for stains on glass (Fig. 8). However, the only fabrics that yielded stain sizes that were statistically different than the glass control were cotton ( $p < 0.03$ ), modal and rayon ( $p < 0.001$ ) at known 30° impact angles, and modal and rayon ( $p < 0.001$ ) at known 10° impact angles. As the final stain shape was often more rectangular than ovalar, overlaying an ellipse was exceptionally difficult for the polyester fabric at the known 30° impact angle (Fig. 4A). Bloodstains on cotton, modal, rayon, and polyester at the known 10° impact angle were easier to assign an elliptical shape, but bloodstains on these materials still demonstrated distorted edges (Fig. 4B-E and Fig. 7B-E), which were excluded from the final elliptical placement. Bloodstains on nylon and glass retained clear elliptical shapes (Fig. 4F-G and Fig. 7F-G).

### 3.3. Angle of impact

When comparing the mean impact angle to the known 30° impact angle, significant departures from the known resulted for poly/span ( $p < 0.001$ ), modal ( $p < 0.001$ ), rayon ( $p < 0.006$ ), and nylon ( $p < 0.003$ ), with the estimated angle of impact consistently measuring less than the known for these fabrics (Fig. 9B). Similarly, for the 10° known angle of impact samples, poly/span ( $p < 0.05$ ), modal ( $p < 0.002$ ), and nylon ( $p < 0.03$ ) substrates also show significant deviations from the known, while rayon did not, and the estimated angle of impact consistently fell below the known angle of impact for these fabrics (Fig. 9A). Within both datasets (10° and 30°), the mean angles of impact were also compared between fabric types and the glass substrate control (Fig. 9). Of the known 30° samples, the mean angles of impact for cotton (29.6°) and glass (28.4°) did not differ from each other. The mean angles of impact for poly/span (19.8°) and modal (22.1°) fabrics also did not differ from each other. However, the angles of impact for cotton and glass were statistically different than poly/span and modal ( $p < 0.01$ ). The mean angle of impact for polyester (26.4°) was in between and, therefore, similar to both of these respective groups. Rayon (26.5°) and nylon (23.5°) were most similar to each other. Rayon was also not statistically different from cotton and glass, while nylon was ( $p < 0.05$ ). Conversely, nylon was also not statistically different from poly/span and modal, while rayon was ( $p < 0.02$ ). In general, there was a tighter range in the mean angles of impact for the known 10° samples (range of 7.3° to 11.2°). The statistical similarities and differences between the fabrics were fairly consistent with what was described for the known 30° samples.

**Table 2**

Descriptive statistics for theoretical 30° and 10° impact bloodstains across substrate types. Elliptical area (mm<sup>2</sup>) and calculated angle of impact (degrees) were determined for each bloodstain, and values were averaged for each substrate type at the specified theoretical impact angle. Calculated angles of impact for each substrate were compared to the theoretical impact angle to determine the percent error, and values were averaged for each fabric type at the specified theoretical impact angle. Relative standard deviation (RSD, %) was derived from the mean calculated angle of impact and the standard deviation for each substrate at a specific impact angle. Five replicates were created on each substrate at both impact angles (four replicates for glass at 30°).

Theoretical Impact Angle	Calculated Parameter	Polyester	Poly/Spin	Cotton	Modal	Rayon	Nylon	Glass
30°	Mean Elliptical Area (mm <sup>2</sup> )*	354.6 (115.0)	203.0 (51.9)	152.6 (43.1)	60.1 (26.2)	76.2 (17.1)	188.9 (32.4)	260.5 (18.8)
	Mean Calculated Angle of Impact (degrees)*	26.4 (9.8)	19.8 (1.9)	29.6 (4.4)	22.1 (2.0)	26.5 (1.5)	23.5 (2.2)	28.4 (3.0)
	Mean Percent Error (%)	29.1	34.1	11.7	26.3	11.7	21.8	9.0
	Relative Standard Deviation (%)	37.1	9.6	14.9	9.0	5.7	9.4	10.6
10°	Mean Elliptical Area (mm <sup>2</sup> )*	454.3 (125.9)	145.5 (17.5)	156.2 (21.0)	84.6 (14.6)	93.1 (35.8)	172.5 (29.9)	225.2 (33.5)
	Mean Calculated Angle of Impact (degrees)*	10.8 (2.3)	8.3 (1.4)	10.4 (1.2)	8.7 (0.4)	11.2 (3.5)	7.3 (1.6)	9.4 (1.2)
	Mean Percent Error (%)	22.0	17.4	9.6	13.2	18.0	27.2	10.2
	Relative Standard Deviation (%)	21.3	16.9	11.5	4.6	31.2	21.9	12.8

\* Values given in parenthesis correspond to the standard deviation (SD)

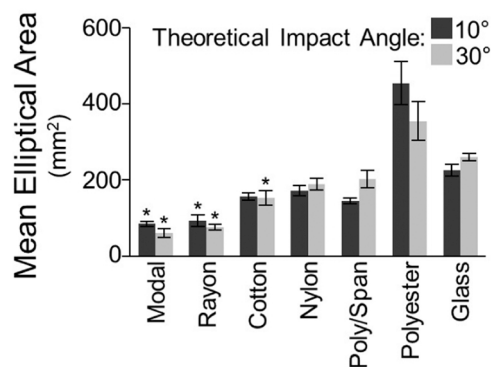


**Fig. 8.** Mean elliptical areas for known 10° (dark grey) and 30° (light grey) impact bloodstains across substrate types. The substrate types (modal, rayon, cotton, nylon, poly/span, polyester, and glass) are shown across the x-axis; the mean elliptical areas measured in mm<sup>2</sup> are plotted on the y-axis. Five replicates per group except for glass at 30°, where  $n = 4$ . Error bars represent the standard error of the mean (SEM). The asterisks (\*) represent statistically significant differences from glass as determined by a Kruskal-Wallis rank sum test followed by a Dunn post hoc analysis (cotton  $p < 0.03$ ; rayon and modal  $p < 0.001$ ).

### 3.4. Precision and accuracy

Bloodstains deposited on rayon at 30° demonstrated the highest precision in the mean angle of impact (5.7 % RSD), and bloodstains deposited on polyester at 30° demonstrated the lowest precision (37.1 % RSD) (Table 2). Relative standard deviation averaged across all seven substrates for the known 10° impacts was higher than the known 30° impacts, 7.1 % and 13.7 %, respectively. The percent error between the estimated angle of impact and the known was used to gauge the accuracy of the measurements. Overall, bloodstains deposited on glass at 30° yielded the smallest percent error (9.0 %), and bloodstains deposited on poly/span at 30° yielded the largest percent error (34.1 %) (Table 2). Percent error averaged across all seven substrates for the known 30° impacts was higher than the known 10° impacts, 20.9 % and 16.8 %, respectively.

### 3.5. Directionality

When evaluated by a certified bloodstain pattern analyst, an opinion regarding directionality was able to be rendered on all glass and nylon bloodstains for both the 10° and 30° datasets. Conversely, an opinion on directionality was only rendered on 8 of 25 total bloodstains across poly/span, cotton, modal, and rayon fabrics for the 30° known angle of

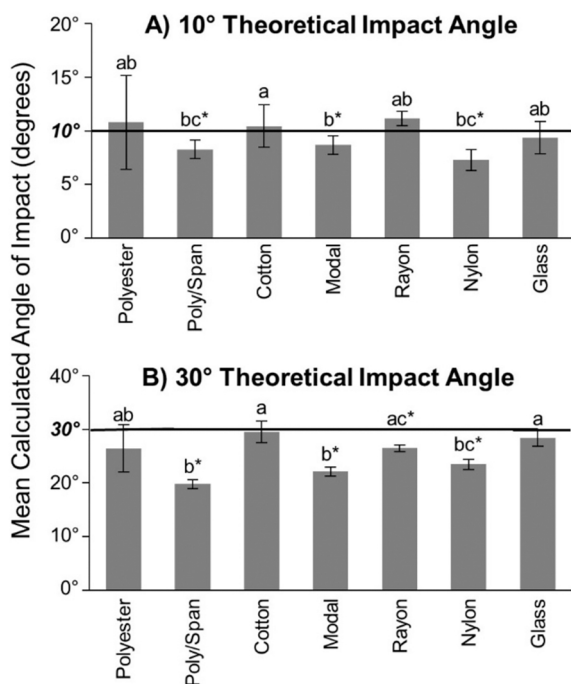


**Fig. 9.** Mean angles of impact for bloodstains across substrate types. A) Blood deposited at a 10° impact angle; B) Blood deposited at a 30° impact angle. The substrate types (polyester, poly/span, cotton, modal, rayon, nylon, and glass) are shown across the x-axis; the mean angles of impact in degrees are plotted on the y-axis. Five replicates per group except for glass at 30, where n = 4. Error bars represent the standard error of the mean (SEM). The horizontal lines represent the known angles of impact (either 10° (top) or 30° (bottom)). The asterisks (\*) represent statistically significant differences from the known impact angle as determined by single sample t-test (p < 0.05). Letter designations represent Dunn post hoc comparisons across the substrate types for bloodstain deposited at either 10° or 30° impact angles; the same letter designation means results are not statistically different; when letter designations differ between groups, p < 0.05.

impact samples. Furthermore, only two polyester and poly/span bloodstains had morphologies suitable for assigning directionality when the fabrics were impacted at a known 10° angle, and no directionality was able to be assigned to any bloodstains on cotton, modal, and rayon

**Table 3**

Contingency table for directionality determination at theoretical 30° and 10° impact angles across substrate types. Columns are divided by substrate type and rows are divided by directionality classification (either classified or not classified). The ‘observed’ values represent number of replicate stains assigned a directionality by a certified bloodstain pattern analyst. The ‘expected’ number of stains were calculated by the equation,  $Expected\ value = \frac{(row\ total \times column\ total)}{total\ observations}$ . A Fisher’s Exact test for independence was used to compare the number of observed directionality classifications to the expected number of classifications across substrates at both theoretical impact angles.

		Theoretical 30° Impacts:						
		Glass	Nylon	Rayon	Modal	Cotton	Poly/Span	Polyester
Observed	Classified:	4	5	1	3	2	2	0
	Not Classified:	0	0	4	2	3	3	5
Expected	Classified:	2	2.5	2.5	2.5	2.5	2.5	2.5
	Not Classified:	2	2.5	2.5	2.5	2.5	2.5	2.5
Fisher’s Exact p-value < 0.008								
		Theoretical 10° Impacts:						
		Glass	Nylon	Rayon	Modal	Cotton	Poly/Span	Polyester
Observed	Classified:	5	5	0	0	0	2	2
	Not Classified:	0	0	5	5	5	3	3
Expected	Classified:	2	2	2	2	2	2	2
	Not Classified:	3	3	3	3	3	3	3
Fisher’s Exact p-value < 0.0001								

fabrics (Table 3). For the stains where directionality was assigned, 100 % of opinions rendered by the certified examiner as to directionality matched the ground-truth of the direction the blood was traveling before impact. When the number of stains assigned a directionality (observed) were compared to the expected across each substrate for both known impact angles (10° and 30°), the ability to assign a directionality was dependent upon the substrate type (p < 0.008), i.e., the substrate type/fabric affects the ability to determine bloodstain directionality (Table 3).

**4. Discussion and conclusions**

The primary finding was that blood interacted with the various fabrics examined (modal, rayon, cotton, nylon, poly/span, and polyester) differently under the same impact conditions depending on fabric type, which created stains of different sizes, shapes, elliptical areas, and angles of impact. Possible explanations for this phenomenon include wicking, fabric thickness, fabric surface roughness, and fabric construction. The expectation that wicking of blood occurs on absorbent substrates and will cause an increase in the bloodstain’s area over time did not necessarily mean that a stain appeared larger than if it impacted on a hard, non-porous surface (glass) under the same impact conditions; modal, rayon, and cotton (cotton only at the known 30° impact angle) generated elliptical areas significantly smaller than elliptical areas on glass. While the elliptical area, as measured here, was not equivalent to the entire bloodstain area, it did provide a consistent way to estimate the stain size. The actual stain size of bloodstains on fabric may be larger than measured by elliptical overlay because the elliptical area does not consider spines, edge distortion, or tails. For example, bloodstains on cotton demonstrated edge distortion.

The modal fabric was noticeably thicker than the other fabrics used, which may account for the smaller stain size as thicker fabrics have been found to generate smaller bloodstains than thinner fabrics [13]. Additionally, absorption of blood vertically into porous materials takes place before radial wicking [1,4]; with a thicker fabric, blood can be displaced more in a vertical direction than in a radial direction, decreasing the outward expansion of the bloodstain. Ridges or folds along the rayon fabric were a prominent feature of that material, which could have disrupted impact and wicking processes. The greater surface roughness of rayon affected the ability of blood to contact and wet the fabric surface. Additionally, the poly/span fabric demonstrated a low degree of wettability as small, spherical blood droplets remained on the fabric’s surface. How a fluid wets and coats a porous surface will influence

subsequent wicking into that material [14]. In the case of poly/span, blood remained on the surface as spherical droplets and did not absorb completely into the fabric. For poly/span, even with little wicking seemingly present, the angle of impact differed significantly compared with both the known impact angle and the estimated angle of impact for the glass substrate. Essentially, the fabric surface may reduce subsequent wicking by changing how blood is able to impact, wet, and coat the surface, leading to a smaller stain size compared to blood interactions on a smoother surface.

Mean impact angles on poly/span, nylon, modal, and rayon (rayon only at the known 30° impact angle) fabrics tended to underestimate the known because of a smaller bloodstain width to length ratio. Gravitational forces may have been working in conjunction with capillary forces to drive the extent of wicking greater in the downwards direction, decreasing the width to length ratio by increasing the bloodstain's elliptical length. However, if this were the case, it would be expected that the estimated impact angles would become more inaccurate as the impact angle became more acute, i.e., going from 30° to 10°, because the gravitational force component parallel to the surface would increase and drive blood wicking more in that direction. Despite this, the accuracy (% error) of the angle of impact was more disparate for the stains deposited at a 30° impact angle (20.9 %) than for the stains deposited at a 10° impact angle (16.8 %). While the effect of gravitational force may be a factor between perpendicular and inclined impacts, further research into fundamental wicking dynamics on inclined surfaces is needed as relevant studies are generally focused on perpendicular impacts [1,4].

Perhaps a better explanation for the estimated angle of impact underestimating the known impact angle for poly/span, modal, and nylon fabrics is that these fabrics were single knit. Single knit fabrics have been shown to demonstrate greater wicking in the wale direction (lengthwise columns of loops) compared to the course direction (crosswise rows of loops) [13]. Here, the elliptical length of the bloodstain followed the wale direction because of how the fabrics were oriented on the drip apparatus and may have led to greater wicking in the lengthwise direction, which could explain the underestimation of the angle of impact for single knit substrates. Similarly, the aforementioned ridges of the rayon fabric may account for an underestimated angle of impact when deposited at 30°, but not 10°. These ridges and folds travelled vertically in the warp direction (lengthwise running yarns). For the bloodstain to grow in the weft direction (crosswise running yarns), blood would have to wick a greater distance (up and down these ridges) in the weft direction than in the warp direction. Therefore, a uniform width to length ratio would not be maintained as more of these ridges were present inside the final bloodstain's width. Due to how blood initially contacts a surface at a 10° impact angle compared to a 30° impact angle, bloodstains impacting at 10° have a smaller width. With fewer ridges that the blood must wick through, the width to length ratio should be more preserved compared to impact on a smooth, non-porous surface.

The estimated angle of impact on cotton and polyester fabrics were not significantly different from the known impact angles despite a greater ability of these fabrics to distort the bloodstain shape over time. By using computer software to draw an ellipse over the bloodstain, the extent to which the ellipse was able to cover the bloodstain without going beyond a given edge was limited. Regarding cotton, occasionally, large areas of the bloodstain's length had to be excluded from the ellipse to ensure the ellipse never went past the bounds of the bloodstain, which might have contributed to the angle of impact estimate on cotton being statistically indistinguishable from the known impact angles. Different outcomes were observed for cotton in research carried out by White [3], who found deviations from the known impact angle as great as 19°. White measured bloodstain length and width by hand rather than by computer, as was done here. Estimated angles of impact on polyester did not differ significantly from the known angles of impact; however, less precision (greater RSD values), was observed compared to the other substrates at both known impact angles. Although calculating an angle

of impact was possible for all fabrics, and the estimate was close to the known angle of impact for certain substrates, the ability to recognize the bloodstain as a drip stain pattern on items of evidence to be able to perform such a calculation is questionable due to the irregular shapes and deviations from the canonical bloodstain morphology. Overall, it seemed that excluding irregular wicking and spurious deviations from an elliptical shape were not enough to yield angles of impact that matched the known impact angle. However, when large portions of the bloodstain had to be excluded from the elliptical selection and angle of impact calculation, such as for cotton and polyester fabrics, the estimated angle of impact was closer to the known impact angle.

Bloodstain shape was different between substrates, affecting the ability to determine directionality. Bloodstain morphology on glass and nylon fabric was consistent with the expected morphology for an impact stain, allowing correct directionality to be assigned for all bloodstains on nylon and glass. Yet, interestingly, the angle of impact differed significantly between the nylon fabric and glass substrates, and the estimated impact angle on nylon was significantly less than the known impact angle. Only a few bloodstains on the other fabrics could be assigned a directionality, and it was determined that the ability to assign directionality was dependent on the substrate. Wicking [1,4,7] and surface roughness [8,14] affect the blood deposition process and subsequent bloodstain shape and may differ between fabrics, which will influence the ability for a directionality to be interpreted. However, when the proper morphology was present, the direction blood was traveling prior to impact could be accurately assigned on various fabrics.

This study is not without limitations. Synthetic blood and porcine blood are perhaps safer more readily available alternatives to human blood for laboratory experimentation, but they present challenges in terms of accuracy and authenticity for the translation of findings to real-world BPA. Therefore, the authors felt it was important to use human blood for this study; however, the safe use of human blood in a research environment presents its own unique challenges pertaining to acquisition and storage such that having a "fresh", unadulterated source is a practical impossibility. The blood supplier used here, Innovative Research, assigns a three-week expiration date, if stored refrigerated, to the human whole blood that was used for this research; therefore, in an effort to ensure stability of the blood, all experimentation was completed within seven days of the blood draw, and the product was stored and handled according to manufacturer recommendations. Additionally, in blood shedding events that require BPA, although it eventually cools to ambient temperature, blood leaving a body is at a temperature that is elevated compared to the surroundings, which presumably has some effect on the fluid dynamics. Other than to allow the blood in this experiment to reach ambient temperature (~70 °F; ~21°C) before use, temperature of the blood was not a controlled factor in this study. Furthermore, the authors acknowledge that blood shedding events are dynamic and the textiles that the blood encounters in the real-world may very well be in motion, have elastic properties or be stretched, may be covering – either more loosely or more taught – more pliable materials than the wooden support that was employed in this study, and are available in a seemingly endless variety of colors, patterns, and compositions. All of these factors may affect the impact, collapse of the blood droplet immediately after impact, and the subsequent wicking, absorption, and final appearance of the bloodstain. However, a crime scene is not a controlled environment, and there are many aspects of the analysis that are unknown or unknowable to the examiner. The primary focus of this work was the expansion of knowledge pertaining to BPA on fabrics, given that the effects of fabric composition on bloodstain formation and morphology have generally been limited to cotton [1,4-6], polyester [7], and denim [8] and that current OSAC guidelines recommend *not* performing any bloodstain pattern analysis on fabrics and porous substrates [15]. The findings presented here demonstrate that while proper morphology for BPA may not always be present with bloodstains on fabrics, some fabrics and circumstances may allow for accurate interpretation given that the proper morphology is present in the stain. There

is clearly a need for further research and the development of guidelines and standards for when bloodstain pattern interpretation on fabric materials and other porous substrates is, and is not, acceptable.

### CRedit authorship contribution statement

**Travis J. Worst:** Writing – review & editing, Supervision, Resources, Methodology. **David M. Hammond:** Supervision, Methodology, Investigation, Conceptualization. **Crystal M Oechsle:** Writing – review & editing, Project administration, Methodology, Formal analysis, Conceptualization. **Dylan J. Drazdik:** Writing – original draft, Investigation, Formal analysis, Data curation.

### Declaration of Competing Interest

The authors declare that they have no known competing financial interests or personal relationships that could have appeared to influence the work reported in this paper

### References

- [1] F. Wang, V. Gallardo, S. Michielsen, T. Fang, Fundamental study of porcine drip bloodstains on fabrics: Blood droplet impact and wicking dynamics, *Forensic Sci. Int.* 318 (2021) 110614, <https://doi.org/10.1016/j.forsciint.2020.110614>.
- [2] S.H. James, P.E. Kish, & T.P. Sutton, *Principles of Bloodstain Pattern Analysis*, Boca Raton, Florida, 2005.
- [3] B. White, Bloodstain patterns on fabrics: the effect of drop volume, dropping height and impact angle, *Can. Soc. Forensic Sci.* 19 (1) (1986) 3–36, <https://doi.org/10.1080/00085030.1986.10757399>.
- [4] X. Li, J. Li, S. Michielsen, Effect of yarn structure on wicking and its impact on bloodstain pattern analysis (BPA) on woven cotton fabrics, *Forensic Sci. Int.* 276 (2017) 41–50, <https://doi.org/10.1016/j.forsciint.2017.04.011>.
- [5] T. de Castro, T. Nickson, D. Carr, C. Knock, Interpreting the formation of bloodstains on selected apparel fabrics, *Int. J. Leg. Med.* 127 (1) (2013) 251–258, <https://doi.org/10.1007/s00414-012-0717-3>.
- [6] E.M.P. Williams, M. Dodds, M.C. Taylor, J. Li, S. Michielsen, Impact dynamics of porcine drip bloodstains on fabrics, *Forensic Sci. Int.* 262 (2016) 66–72, <https://doi.org/10.1016/j.forsciint.2016.02.037>.
- [7] T.C. de Castro, D.J. Carr, M.C. Taylor, J.A. Kieser, W. Duncan, Drip bloodstain appearance on inclined apparel fabrics: Effect of prior-laundrying, fiber content and fabric structure, *Forensic Sci. Int.* 266 (2016) 488–501, <https://doi.org/10.1016/j.forsciint.2016.07.008>.
- [8] H.F. Miles, R.M. Morgan, J.E. Millington, The influence of fabric surface characteristics on satellite bloodstain morphology, *Sci. Justice* 54 (4) (2014) 262–266, <https://doi.org/10.1016/j.scijus.2014.04.002>.
- [9] M.C. Taylor, T.L. Laber, P.E. Kish, G. Owens, N.K.P. Osborne, The Reliability of Pattern Classification in Bloodstain Pattern Analysis—PART 2: Bloodstain Patterns on Fabric Surfaces, *J. Forensic Sci.* 61 (6) (2016) 1461–1466, <https://doi.org/10.1111/1556-4029.13191>.
- [10] National Institute of Standards and Technology (NIST) Organization of Scientific Area Committees (OSAC) Bloodstain Pattern Analysis (BPA) Subcommittee, Differentiating spatter from transfer for blood deposited on textiles. ([https://www.nist.gov/system/files/documents/2021/05/17/BPA%20SC\\_R%26D%20Need\\_Differentiating%20spatter%20from%20transfer%20on%20textiles%202021.pdf](https://www.nist.gov/system/files/documents/2021/05/17/BPA%20SC_R%26D%20Need_Differentiating%20spatter%20from%20transfer%20on%20textiles%202021.pdf)), approved 1 March 2021 (accessed 6 March 2024).
- [11] National Institute of Standards and Technology (NIST) Organization of Scientific Area Committees (OSAC) Bloodstain Pattern Analysis (BPA) Subcommittee, Addendum to the Research Needs Assessment Form: Research questions regarding differentiating spatter from transfer for blood deposited on textiles. ([https://www.nist.gov/system/files/documents/2021/05/17/BPA%20SC\\_R%26D%20Need\\_Differentiating%20spatter%20from%20transfer%20on%20textiles%202021\\_ADDENDUM.pdf](https://www.nist.gov/system/files/documents/2021/05/17/BPA%20SC_R%26D%20Need_Differentiating%20spatter%20from%20transfer%20on%20textiles%202021_ADDENDUM.pdf)), approved 1 March 2021 (accessed 6 March 2024).
- [12] J.Y.M. Chang, S. Michielsen, Effect of fabric mounting method and backing material on bloodstain patterns of drip stains on textiles, *Int. J. Leg. Med.* 130 (3) (2016) 649–659, <https://doi.org/10.1007/s00414-015-1314-z>.
- [13] R. Baby, S. Michielsen, J. Wu, Effects of yarn size and blood drop size on wicking and bloodstains in textiles, *J. Forensic Sci.* 66 (4) (2021) 1246–1256, <https://doi.org/10.1111/1556-4029.14702>.
- [14] E. Kissa, Wetting and Wicking, *Text. Res. J.* 66 (10) (1996) 660–668, <https://doi.org/10.1177/004051759606601008>.
- [15] National Institute of Standards and Technology (NIST) Organization of Scientific Area Committees (OSAC) Bloodstain Pattern Analysis (BPA) Subcommittee, Bloodstain Classification Process Map, Version 2.3. ([https://www.nist.gov/system/files/documents/2020/05/19/BPA%20Process%20Map\\_Dec2019.pdf](https://www.nist.gov/system/files/documents/2020/05/19/BPA%20Process%20Map_Dec2019.pdf)), 2019 (accessed 7 March 2024).